KSME

Springer

Journal of Mechanical Science and Technology 34 (3) 2020

Original Article
DOI 10.1007/s12206-020-0201-9

Keywords:
· Drilling
· Downhole tool
· Dynamics
· Stick-slip
· Vibration
· Drill string

Correspondence to:
Jialin Tian
tianjialin001@gmail.com
Lai Wei
1364845946@qq.com

Citation:
Tian, J., Wei. L., Yang, L., Dai, L., Zhang, T., Liu, H. (2020). Research and experimental analysis of drill string dynamics characteristics and stick-slip reduction mechanism. Journal of Mechanical Science and Technology 34 (3) (2020) 977~986.
http://doi.org/10.1007/s12206-020-0201-9

Received May 16th, 2019
Revised October 15th, 2019
Accepted January 7th, 2020

† Recommended by Editor No-cheol Park

Research and experimental analysis of drill string dynamics characteristics and stick-slip reduction mechanism

Jialin Tian[1,2], Lai Wei[1], Lin Yang[1], Liming Dai[3], Tangjia Zhang[1] and He Liu[4]

[1]Schools of Mechatronic Engineering, Southwest Petroleum University, Chengdu, 610500, China, [2]School of Mechanical Engineering, Southwest Jiaotong University, Chengdu 610031, China, [3]Industrial Systems Engineering, University of Regina, Regina, SK S4S 0A2, Canada, [4]CNPC Bohai Drilling Engineering Company Limited, Tianjin, 300000, China

Abstract Stick-slip of the drill string, as one of the critical factors affecting drilling efficiency, has always been a hot topic for experts and scholars in related fields. Serious stick-slip vibration affects the well construction efficiency, drilling cost and even lead to a downhole accident. Therefore, based on the current research, this paper takes a new type of composite vibration tool as the research object, studies the working mechanism of the tool and analyzes the effect of stick-slip reduction. After establishing the multi-degree-of-freedom torsional dynamics model, we obtained the results of torsional vibration dynamics by cases analysis based on working conditions and related mechanical parameters. In addition, the results of the examples, compared with the field experimental data, verify that the vibration shock generated by the new composite tool can effectively reduce the torque fluctuation range of the system, avoid the occurrence of stick-slip phenomenon, improve the ROP (rate of penetration), and make drilling process more stable. This paper can provide reference for the optimization and development of stick-slip technology in drilling engineering, and the theoretical methods can also be developed to study the dynamics of drill string.

1. Introduction

The oil and gas resources play an important role in the development of society, which has both a direct and indirect impact on the economy or industry [1-4]. The drilling of oil and gas, however, faces more and more challenges since modern drilling has gradually developed into special process wells such as large displacement wells and ultra-deep wells [5-8]. During the drilling of these complex process wells, stick-slip phenomenon occurs frequently. Severe stick-slip phenomenon can lead to premature failure of the BHA (bottom hole assembly) and even cause downhole safety accidents, affecting the drilling rate and drilling efficiency, causing severe economic losses [9-12]. Therefore, the study of the stick-slip theory of the drill string and the research of reducing stick-slip technology are of great significance for improving the drilling speed and production efficiency. Experts and scholars in related fields have done a lot of research on the stick-slip and achieved corresponding results [13-15]. In the 1980s, Kyllingstad et al. proposed a mathematical model of stick-slip vibration [16, 17], found that when the stick-slip vibration occurred, the drilling performance was worse than that of conventional drilling. Cull et al. in 1999 showed that the main cause of stick-slip phenomenon in the downhole drill string system is the mutual friction between the drill bit and the bottom of the well [18, 19]. The physical and mathematical model is established to analyze the downhole friction into two types: Continuous friction and discontinuous friction forms. Navarro-Lopez and Suarez modeled the torsional behavior of the drill string and proposed a control scheme to help reduce stick-slip in 2004 [20, 21]. The control method is a decentralized control method, that is, the angular velocity of the top end of the drill string and the bit speed are separately controlled. Eva et al. in 2009 proposed an alternative method to characterize the stick-slip vibration and other bit viscous problems in drilling systems and designed a proportional-integral controller to reduce the stick-slip of the drill string [22]. In 2014, Kovalyshen et al. studied the causes of stick-slip vibration and performed linear stability analysis of coupled axial torsional vibrations. In 2018, Tian et al. used a constant torque tool as the carrier to establish a longitudinal-torsion coupled stick-slip dynamics model and obtained the longitudinal and torsional dynamics of the drill bit [23-25]. Although these studies are of the important reference value for further research on related technologies or optimization design, most of the previous studies are only for theoretical research, lack of experimental verification, which becomes a factor restricting the technological applications. And the current research method does not combine the drill string with the drill bit for analysis.

Based on the theory research of drill string dynamics, we designed a new type of composite vibration tool combined with design parameters, working parameters and related mechanical calculations, then established the torsional vibration of the drill string model based on the actual working conditions [26, 27]. Through the developed model, combined with the specific parameters of the tool, we can get the angular velocity and displacement results, torque results of the system and phase diagram of drill bit. Then the field test was used to verify the feasibility of the theoretical model and the correctness of the example. In addition, we compare the obtained field experimental data with the results of the example to analyze the effect of stick-slip reduction and speed increasing. The results show that the composite vibration tool can effectively reduce the stick-slip and improve the ROP, and the research method can provide a reference for the in-depth study of similar drill string dynamics, bit rock breaking, and friction reduction.

2. Theoretical model

Fig. 1 shows the structure of the new composite vibration tool, which consists mainly of the upper joint, the upper radial bearing, the turbine stator the rotor system, the turbine housing, the turbine drive shaft, the lower radial bearing, and the disc-valve impact system. Fig. 2 shows disk-valve impact system which is the core part of the tool. The working principle is as follows: high-pressure drilling fluid flows into the inside of the tool, then passes through the turbine stator the rotor system, driving the turbine drive shaft to rotate, then the turbine drive shaft drives the disc valve to rotate continuously periodically. Due to the structural characteristics of the moving and static disc valve, the overcurrent area of the drilling fluid changes regularly during the rotation, thereby generating a periodic axial force. Then, high-pressure drilling fluid flows from the overflow passage into the impact chamber to impact the hammer so that the hammer rotates against the impact seat to generate a torsional impact force inside of the tool. The high and low pressure changes inside the chamber cause the device to make a periodic circumferential impact.

To study the dynamic characteristics of the new tool and the mechanism of reducing stick-slip, we make the following as-

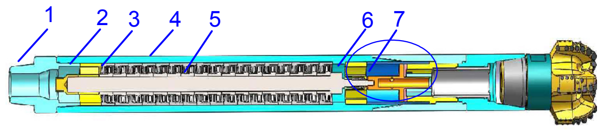

Fig. 1. Schematic diagram of the new composite vibration tool (1. Upper joint, 2. Upper radial bearing, 3. Turbo stator and rotor system, 4. Turbine housing, 5. Turbine drive shaft, 6. Lower radial bearing, 7. Disc-valve impact system).

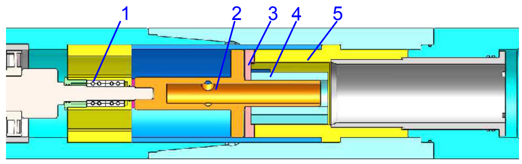

Fig. 2. Disk-valve impact system (1. Lower radial bearing, 2. Moving disc valve, 3. Static disc valve, 4. Impact hammer, 5. Impact seat).

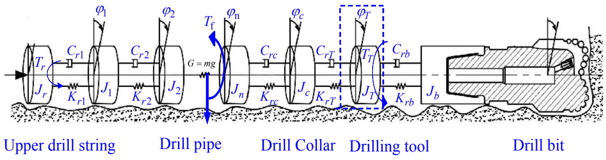

Fig. 3. Torsional vibration model of the drill string system.

sumptions based on actual working conditions, elastic mechanics, linear and nonlinear dynamics, etc. to establish a multi-degree-of-freedom torsional vibration model of the drill string [28-31], as shown in Fig. 3.

(1) It is assumed that the drill pipe, drill collar, drill bit, etc. belong to the drill string system, the whole system and the new composite vibration tool are small elastic deformed bodies with uniform mass distribution.

(2) Assuming that the studied horizontal well section is long enough to ignore the influence of the upper boundary conditions on vibration transmission.

(3) Assuming that the drill string system is in regular contact with the wellbore, the positive pressure generated by the drill string system, the gravity, frictional forces, and frictional torque evenly distributed while ignoring the process of mutual transformation of static and dynamic friction of each node during drilling.

(4) Ignoring the effects of temperature changes caused by lateral vibration of the drill string system and changes in the buoyancy of the drilling fluid.

Discretizing the torsional vibration model based on the model of Fig. 3 and dividing the drill string into n nodes, each drill string unit has a moment of inertia J_i (i = 1,2,…,n,c,T,b; $c = n + 1$, $T = n + 2$, $b = n+3$). The equivalent moment of inertia of the drill collar is J_c; the vibrating tool is J_T, the drill bit is J_b, and the spring having a torsional stiffness K_{ri} and a torsional damping C_{ri} connects the mass units. The input torque of the entire drill string system is T_m, T_{ab} to the viscous torque of the drill bit, T_{fb} to the friction torque, T_T to the impact torque generated by the tool in the drill string system, and T_f to the bottom hole friction

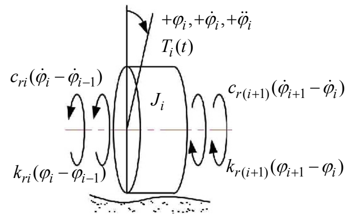

Fig. 4. Single mass torsion motion model.

torque. For the drilling fluid is hugely complicated in the circulation of the wellbore, this paper mainly analyzes the torsional stick-slip phenomenon at the drill bit and ignores the influence of the drilling fluid's viscous torque on the drill pipe.

Selecting the appropriate coordinate system and using $\varphi_i(t)$ to indicate the position coordinates of the i-th node from the equilibrium position. Selecting the node J_i for stress analysis (Fig. 4) and the differential equation of motion can be derived for the node model.

$$\begin{aligned} & J_i\ddot{\varphi}_i - c_{ri}\dot{\varphi}_{i-1} + (c_{ri} + c_{r(i+1)})\dot{\varphi}_i - c_{r(i+1)}\dot{\varphi}_{i+1} - \\ & k_{ri}\varphi_{i-1} + (k_{ri} + k_{r(i+1)})\varphi_i - k_{r(i+1)}\varphi_{i+1} = T_i \\ & i = 1,2,3,\cdots,n,\mathrm{c},\mathrm{T},b \end{aligned} \tag{1}$$

When $i = 1$, $\varphi_0 = 0$ and $i = b$, $\varphi_{b+1} = 0$, according to Eq. (1), differential equations of motion can be derived respectively, according to Eq. (1).

$$\begin{aligned} & J_1\ddot{\varphi}_1 + (c_{r1} + c_{r2})\dot{\varphi}_1 - \\ & c_{r2}\dot{\varphi}_2 + (k_{r1} + k_{r2})\varphi_1 - k_{r2}\varphi_2 = T_1 \end{aligned} \tag{2}$$

$$\begin{aligned} & J_b\ddot{\varphi}_b - c_{rb}\dot{\varphi}_{b-1} + (c_{rb} + c_{r(b+1)})\dot{\varphi}_b - \\ & k_{rb}\varphi_{b-1} + (k_{rb} + k_{r(b+1)})\varphi_b = T_b \end{aligned} \tag{3}$$

The differential equations of the drill string system with or without tool are respectively established to compare and analyze the stick-slip effect of the composite vibration tool. However, since the difference between the dynamic model with and without tool lies in the tool mass block J_z, the tool part is removed from the dynamic model of the drill string system with tool, that is, the dynamic equation without tool is obtained, and the drill string system equation with tool is analyzed here. By combining Eqs. (1)-(3) and the torsion motion model in Fig. 4, we can obtain the general motion differential equation expressed by the tool in matrix form:

$$\mathbf{J}\ddot{\varphi}(t) + \mathbf{C}_r\dot{\varphi}(t) + \mathbf{K}_r\varphi(t) = \mathbf{T}(t) \tag{4}$$

where the moment of inertia matrix, torsional damping matrix, and torsional stiffness matrix respectively show as following:

$$\mathbf{J} = \begin{bmatrix} J_1 & & & & & & \\ & J_2 & & & & & \\ & & \ddots & & & & \\ & & & J_n & & & \\ & & & & J_c & & \\ & & & & & J_T & \\ & & & & & & J_b \end{bmatrix} \tag{5}$$

$$\mathbf{C}_r = \begin{bmatrix} c_{r1}+c_{r2} & -c_{r2} & & & & & \\ -c_{r2} & c_{r2}+c_{r3} & & & & & \\ & & \ddots & & & & \\ & & & c_{rn}+c_{rc} & -c_{rc} & & \\ & & & -c_{rc} & c_{rc}+c_{rT} & -c_{rT} & \\ & & & & -c_{rT} & c_{rT}+c_{rb} & -c_{rb} \\ & & & & & -c_{rb} & c_{rb}+c_{r(b+1)} \end{bmatrix} \tag{6}$$

$$\mathbf{K}_r = \begin{bmatrix} k_{r1}+k_{r2} & -k_{r2} & & & & & \\ -k_{r2} & k_{r2}+k_{r3} & & & & & \\ & \ddots & \ddots & & & & \\ & & & k_{rn}+k_{rc} & -k_{rc} & & \\ & & & -k_{rc} & k_{rc}+k_{rT} & -k_{rT} & \\ & & & & -k_{rT} & k_{rT}+k_{rb} & -k_{rb} \\ & & & & & -k_{rb} & k_{rb}+k_{r(b+1)} \end{bmatrix} \tag{7}$$

The initial condition for the torsional vibration of the drill string system is

$$\begin{aligned} & \varphi_i(t=0) = 0 \\ & \dot{\varphi}_i(t=0) = 0 \\ & \ddot{\varphi}_i(t=0) = 0 \end{aligned} \tag{8}$$

The boundary conditions of the drill string system are known from the torsional vibration model. For the left boundary, since the upper boundaries conditions are simplified, the external torques at the first node are the system input torque T_m and the friction torque T_{f1}:

$$T_1(t) = T_m - F_{f1} \tag{9}$$

Friction torque is:

$$\begin{cases} T_{\mathrm{fi}} = \mu_{\mathrm{i}} F_{N\mathrm{i}} R_{\mathrm{i}} \\ F_{N\mathrm{i}} = m_{\mathrm{i}} g \end{cases} \tag{10}$$

According to the boundary conditions, the vector $\varphi(t)$, vector $\dot{\varphi}(t)$, vector $\ddot{\varphi}(t)$ and moment vector $\mathbf{T}(t)$ in Eq. (4) are expressed as:

$$\varphi(t) = \begin{bmatrix} \varphi_1(t) \\ \varphi_2(t) \\ \vdots \\ \varphi_n(t) \\ \varphi_c(t) \\ \varphi_T(t) \\ \varphi_b(t) \end{bmatrix},\ \dot{\varphi}(t) = \begin{bmatrix} \dot{\varphi}_1(t) \\ \dot{\varphi}_2(t) \\ \vdots \\ \dot{\varphi}_n(t) \\ \dot{\varphi}_c(t) \\ \dot{\varphi}_T(t) \\ \dot{\varphi}_b(t) \end{bmatrix},\ \ddot{\varphi}(t) = \begin{bmatrix} \ddot{\varphi}_1(t) \\ \ddot{\varphi}_2(t) \\ \vdots \\ \ddot{\varphi}_n(t) \\ \ddot{\varphi}_c(t) \\ \ddot{\varphi}_T(t) \\ \ddot{\varphi}_b(t) \end{bmatrix},\ \mathbf{T}(t) = \begin{bmatrix} T_m - T_{f1}(t) \\ -T_{f2}(t) \\ \vdots \\ -T_{fn}(t) \\ 0 \\ T_T \\ -T_{fb} \end{bmatrix} \tag{11}$$

The equivalent moment of inertia of the mass of the torsional vibration drill string system is expressed as:

$$J_i = \rho \frac{\pi l_i}{32}(D_i^2 - d_i^2) \tag{12}$$

where ρ is the density of the drill string material, kg/m^3; D_i is the outer diameter of the drill pipe, mm; d_i is the inner diameter of the drill pipe, mm; l_i is the length of the i-th node, mm.

The torsional stiffness K_{ri} between the masses of the torsional vibration drill string system can be expressed:

$$k_{ri} = \frac{\pi G_i (D_i^4 - d_i^4)}{32 l_i} \tag{13}$$

where G_i is the material shear modulus of the drill string system, Mpa.

The torsional damping C_{ri} between the masses of the drill string system is expressed as:

$$c_{ri} = \frac{\xi_{ri} l_i}{3} \tag{14}$$

where ξ_{ri} is the torsional damping coefficient per unit length of the drill string, Ns/rad·.

Defining system state vector $\mathbf{z}'$:

$$\begin{aligned}\mathbf{z}' &= (\varphi_1, \dot{\varphi}_1, \varphi_2, \dot{\varphi}_2, \cdots, \varphi_n, \dot{\varphi}_n, \varphi_c, \dot{\varphi}_c, \varphi_T, \dot{\varphi}_T, \varphi_b, \dot{\varphi}_b)^T \\ &= (z_1, z_2, z_3, z_4, \cdots, z_{m-1}, z_m, z_{m+1}, z_{m+2}, z_{m+3}, z_{m+4}, z_{m+5}, z_{m+6})^T\end{aligned} \tag{15}$$

where m = $2n$ is the system state order. Since the drill collar, the vibration tool, and the drill bit mass exist, the state order vector of the tool-less system is m+6.

According to Eq. (14), the dynamic Eq. (4) of the drill string system is reduced to obtain the state space equations of the drill string system.

$$\begin{cases} \dot{z}_1 = z_2 \\ \dot{z}_2 = -\dfrac{(c_{r1}+c_{r2})}{J_1} z_2 + \dfrac{c_{r2}}{J_1} z_4 - \dfrac{(k_{r1}+k_{r2})}{J_1} z_1 + \dfrac{k_{r2}}{J_1} z_3 + \dfrac{T_m \text{-} T_1}{J_1} \\ \dot{z}_3 = z_4 \\ \vdots \\ \dot{z}_{m\text{-}1} = z_m \\ \dot{z}_m = \dfrac{c_{rn}}{J_n} z_{m\text{-}2} - \dfrac{(c_{rn}+c_{r(n+1)})}{J_n} z_m + \dfrac{c_{r(n+1)}}{J_n} z_{m+2} + \dfrac{k_{rn}}{J_n} z_{m\text{-}1} - \dfrac{(k_{rn}+k_{r(n+1)})}{J_n} z_{m+1} + \dfrac{k_{r(n+1)}}{J_n} z_{m+3} - \dfrac{T_n}{J_n} \\ \vdots \\ \dot{z}_{m+6} = \dfrac{c_{rb}}{J_b} z_{m+4} - \dfrac{(c_{rb}+c_{r(b+1)})}{J_b} z_{m+6} + \dfrac{k_{rb}}{J_b} z_{m+3} - \dfrac{(k_{rb}+k_{r(b+1)})}{J_b} z_{m+5} - \dfrac{T_{fb}}{J_b} \end{cases} \tag{16}$$

Simplify it into a matrix form:

$$\dot{\mathbf{z}} = \mathbf{X} z(t) + \mathbf{Y} w + \mathbf{T}(z(t)) \tag{17}$$

where w = T_m is the torsion input of the system, and the state matrices **X'**, **Y'** and **T'** are respectively expressed as follows:

$$\mathbf{X} = \begin{bmatrix} 0 & 1 & 0 & 0 & \cdots & 0 & 0 & 0 & 0 & 0 & 0 \\ -\frac{(k_{r1}+k_{r2})}{J_1} & -\frac{(c_{r1}+c_{r2})}{J_1} & \frac{k_{r2}}{J_1} & \frac{c_{r2}}{J_1} & \cdots & 0 & 0 & 0 & 0 & 0 & 0 \\ 0 & 0 & 0 & 1 & \cdots & 0 & 0 & 0 & 0 & 0 & 0 \\ \frac{k_{r2}}{J_2} & \frac{c_{r2}}{J_2} & -\frac{(k_{r2}+k_{r3})}{J_2} & -\frac{(c_{r2}+c_{r3})}{J_2} & \cdots & 0 & 0 & 0 & 0 & 0 & 0 \\ \vdots & \vdots & \vdots & \vdots & \ddots & \vdots & \vdots & \vdots & \vdots & \vdots & \vdots \\ 0 & 0 & 0 & 0 & \cdots & 0 & 1 & 0 & 0 & 0 & 0 \\ 0 & 0 & 0 & 0 & \cdots & -\frac{(k_{rc}+k_{rT})}{J_c} & -\frac{(c_{rc}+c_{rT})}{J_c} & \frac{k_{rT}}{J_c} & \frac{c_{rT}}{J_c} & 0 & 0 \\ 0 & 0 & 0 & 0 & \cdots & 0 & 0 & 0 & 1 & 0 & 0 \\ 0 & 0 & 0 & 0 & \cdots & \frac{k_{rT}}{J_T} & \frac{c_{rT}}{J_T} & -\frac{(k_{rT}+k_{rb})}{J_T} & -\frac{(c_{rT}+c_{rb})}{J_T} & \frac{k_{rb}}{J_T} & \frac{c_{rb}}{J_T} \\ 0 & 0 & 0 & 0 & \cdots & 0 & 0 & 0 & 0 & 0 & 1 \\ 0 & 0 & 0 & 0 & \cdots & 0 & 0 & \frac{k_{rb}}{J_b} & \frac{c_{rb}}{J_b} & -\frac{(k_{rb}+k_{r(b+1)})}{J_b} & -\frac{(c_{rb}+c_{r(b+1)})}{J_b} \end{bmatrix} \tag{18}$$

$$\mathbf{Y} = \begin{bmatrix} 0 & \frac{1}{J_m} & 0 & 0 & \cdots & 0 & 0 & 0 & 0 & 0 & 0 \end{bmatrix} \tag{19}$$

$$\mathbf{T}(x(t)) = \begin{bmatrix} 0 & \frac{T_m - T_1}{J_1} & 0 & -\frac{T_2}{J_2} & \cdots & 0 & 0 & 0 & \frac{T_T}{J_T} & 0 & -\frac{T_{fb}}{J_b} \end{bmatrix} \tag{20}$$

Furthermore, Karnopp friction model between dynamic and static models is adopted for the friction at the bit [32], and the friction torque is:

$$T_{fb}(\omega_b) = \begin{cases} T_{mb} & |\omega_b| < \omega_0, |T_{mb}| \le T_{fs} \\ T_{fs} sgn(\omega_b) & |\omega_b| < \omega_0, |T_{mb}| > T_{fs} \\ \left(T_{fc} + (T_{fs} - T_{fc}) e^{[-(\omega_b/\omega_s)^{\delta}]} + T_{\mu b}\right) sgn(\omega_b) & \text{others} \end{cases} \tag{21}$$

where $\boldsymbol{T}_{mb}$ is the driving torque of the drill string system, Nm; ω_0 is the critical speed of dynamic and static friction, $\omega_0 > 0$; ω_b is the angular velocity of the drill bit, rad/s; $sgn(\omega_b)$ is the judgment function, and the bit is rotated clockwise to be positive.

Drill drive torque is:

$$T_{mb} = c_{rb}(\dot{\varphi}_c - \dot{\varphi}_b) + k_{rb}(\varphi_c - \varphi_b) - c_{r(b+1)} \dot{\varphi}_b \tag{22}$$

3. Analysis of example

According to the torsional vibration model of the drill string system established above, combined with the specific parameters listed in Table 1, the torsional stick-slip vibration results of the drilling system with or without the new type of composite vibration tool are obtained, and the specific example results are as follows.

3.1 Angular velocity and displacement results

Fig. 5 shows the angular velocity and angular displacement of stick-slip vibration of each component in the drill string system without the new composite vibration tool. As can be seen from Fig. 5(a), within t = 7.3 s, the drill pipe rotates normally, and its maximum angular velocity reaches 7.4 rad/s. Since the driving torque received at the initial moment of the drill bit is insufficient to overcome the friction torque at the bottom of the well, the angular velocity of the drill bit is 0 in 7.3 s, at a viscous state. The drill string system begins to twist and accumulate

Table 1. Example parameters of drill string system.

Parameter name	Values
Input static drilling pressure W_{ob} (KN)	100
Input torque T_m (Nm)	10000
Drill pipe outer diameter D_i (mm)	114.3
Drill pipe inner diameter d_i (m)	97.18
Unit drill pipe length l_i （m）	10
Drill pipe material density ρ (kg/m^3)	7850
Moment of inertia of the drill pipe J_i (kg ·m^2)	2465.2
Shear modulus of drill string G (Pa)	8.6e10
Torsional damping factor per unit length of drill string ξ_{ri}	0.2
Torsional stiffness between drill pipe and drill collar k_{ci} (Nm/rad)	980
Torsional stiffness between drill collar and tool k_{cT} (Nm/rad)	865
Torsional stiffness between tool and drill bit k_{cb} (Nm/rad)	830
Torsional stiffness between drill bit and rock $k_{c(b+1)}$ (Nm/rad)	224
Torsional damping between drill pipe joints c_{ri} (Nms/rad)	135.6
Torsional damping between drill pipe and drill collar c_{rc} (Nms/rad)	185
Torsional damping between drill collar and tool c_{rT} (Nms/rad)	146
Torsional damping between drill collar and drill bit c_{rb} (Nms/rad)	168
Torsional damping between drill bit and rock $C_{r(b+1)}$ (Nms/rad)	76

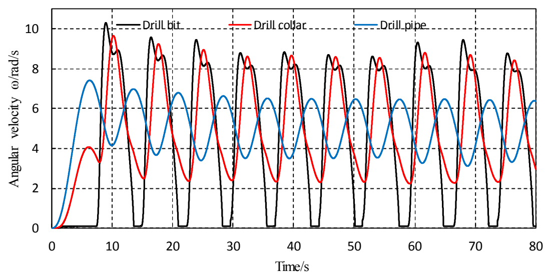

(a) Angular velocity results

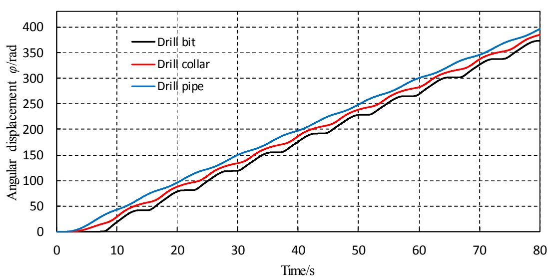

(b) Angular displacement results

Fig. 5. Results of stick-slip vibration of various components of drill string system without tool.

energy at t = 0. When the driving torque on the drill bit is higher than the bottom hole friction torque, the angular velocity of the drill bit increases rapidly from 0 to 10.17 rad/s. Since then, due to the release of energy, the driving torque on the bit gradually decreases, and the angular velocity of the bit gradually decreases under the action of friction torque, fluctuating between 0 and the maximum value, which is called slip state, and the whole viscous slip state is a stick-slip process. The movement rule of drill collar and drill pipe under the influence of stick-slip is shown in Fig. 5.

Fig. 5(b) shows the angular displacement of the drill string system. Bit also exhibits a stick-slip phenomenon at t = 7.3 s, and it can be seen that the angular displacement of the drill bit always lags behind that of the drill pipe.

For comparison, Fig. 6 shows the motion results of the components of the drill string system after the addition of the new composite vibration tool. Comparing Figs. 6(a) and 5(a), it can be found that the angular velocity is almost the same in t = 7.3 s, the angular velocity of the drill pipe, drill collar and drill string increases from 0, and the maximum angular velocity of the drill pipe reaches 7.7 rad/s. The drill bit rotated from 5.5 s due to the friction torque of the bottom hole, and the angular velocity increased from 0 to a maximum angular velocity of 9.2 rad/s, and then gradually decreased to the minimum angular velocity of 1.44 rad/s under the action of bottom hole friction torque. Also, the amplitude of angular velocity fluctuation decreased significantly, and no stick-slip phenomenon occurs in the system. Finally, the angular velocity fluctuations of various components of the drill string system gradually become stable over time. Moreover, the angular displacement of the drill bit gradually increases with time, and there is no case where the angular displacement remains unchanged, meaning that there is no stick-slip phenomenon.

It can be seen from Figs. 6 and 7, that the drill string system with the new composite vibration tool has no stick-slip phenomenon during the drilling process, which reduces the fluctuation amplitude of the bit angular velocity so that the drilling process can run smoothly.

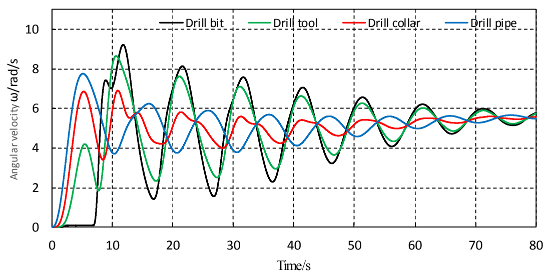

(a) Angular velocity results

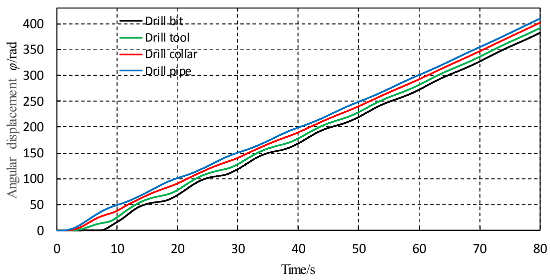

(b) Angular displacement results

Fig. 6. Results of stick-slip vibration of various components of drill string system with tool.

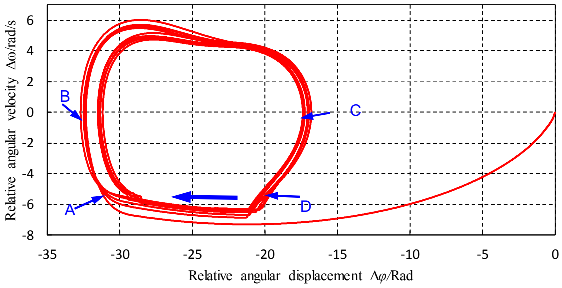

(a) Phase diagram of drill bit relative motion

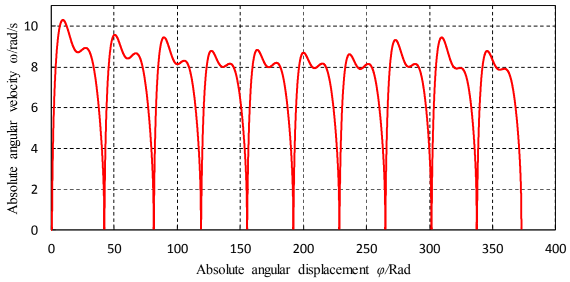

(b) Phase diagram of drill bit absolute motion

Fig. 7. Phase diagram of drill bit movement without tool.

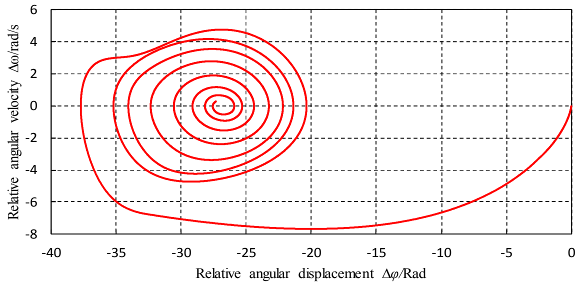

(a) Phase diagram of drill bit relative motion

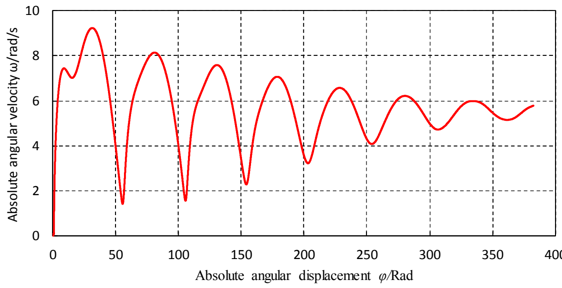

(b) Phase diagram of drill bit absolute motion

Fig. 8. Phase diagram of drill bit movement with tool.

3.2 Phase diagram analysis

According to the variation law of the angular velocity and angular displacement of the drill string system, we obtained the phase diagram of the drill bit with/without the tool (Figs. 7 and 8) to reflect the stability of the drill string system. In Fig. 7(a), the trajectory of the relative motion phase of the bit converges to the stability limit cycle in the phase plane, indicating that stick-slip vibration occurs in the drill string system. At the initial moment, both the drill bit and the drill pipe are stationary, and the relative angular displacement and relative angular velocity of the drill bit are 0. As the movement of the drill bit lags behind that of the drill pipe, relative movement occurs between the drill bit and the drill pipe. When the drill bit enters the slip state from the viscous state (point A in Fig. 7(a)), the relative angular velocity of the drill bit decreases to 0, and the relative angular displacement reaches the maximum value (point B in the Fig. 7(a)). After that, from point B to point C, the angular velocity of the bit alternates with the angular velocity of the drill pipe until it moves to point D, and the bit enters the viscous state again. From point D to point A, the angular velocity of the bit is 0, and the bit remains viscous until point A is broken through and enters the next slip state. The entire stick-slip process presents a closed limit cycle in the relative motion phase diagram of the drill bit, and the bit has periodic stick-slip vibration.

In Fig. 7(b), when there is no tool, the angular velocity of the bit gradually increases from 0 to the maximum value and then drops to the minimum value 0. When the absolute angular velocity of the drill bit is 0, the drill bit is in a viscous state during this process.

When the angular velocity of the bit is greater than 0, the bit is in the slip stage. As the drill bit rotates, the angular displacement gradually increases, and the bit phase trajectory gradually moves to the right. At the same time, the absolute angular velocity of the drill bit presents a periodic change, and the vibration has no attenuation trend.

When there is a tool (Fig. 8), the relative motion phase trajectory of the drill bit is a spiral curve that gradually converges, and the final relative angular velocity of the movement tends to 0. That is, the angular velocity of the drill bit increasingly tends to be equal to that of the drill pipe, maintains a steady movement. In the process, there is no stick-slip vibration occurs. The trajectory curve of the absolute phase of the drill is attenuated and eventually tends to be stable, which means that the absolute angular velocity of the drill bit is a stable value, no stick-slip phenomenon occurs.

It can be seen from the comparison of Figs. 7 and 8 that when there is no new composite vibration tool in the drill string system, the relative motion phase diagram of the drill bit is a periodic limit cycle, and the absolute angular displacement of the drill bit changes periodically, resulting in stick-slip vibration. When the new composite vibration tool is added to the drill string system, the relative motion phase diagram of the drill bit is spiral and eventually stabilizes. The amplitude of the absolute angular velocity fluctuation of the drill bit gradually attenuates and tends to be stable, and no stick-slip phenomenon occurs.

3.3 Torque results analysis

Comparing Figs. 9(a) and (b), it is found that when there is

Table 2. Main structural parameters of the tool.

Parameters	Values
Tool type (mm)	172
Total length of tool (mm)	2100
Disc valve hole outer diameter (mm)	60
Disc valve bore diameter (mm)	35
Total length of impact hammer (mm)	120
Impact hammer outer diameter (mm)	135
Impact hammer inner diameter (mm)	65
Total length of the impact seat (mm)	265
Impact seat outer diameter (mm)	135
Impact seat inner diameter (mm)	95

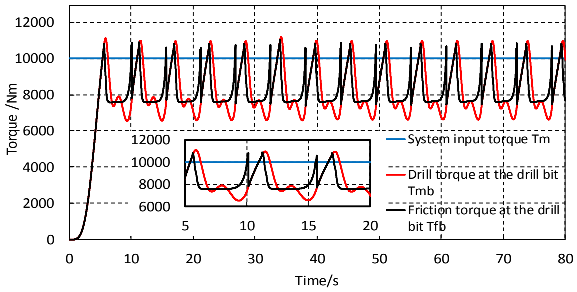

(a) Without tool

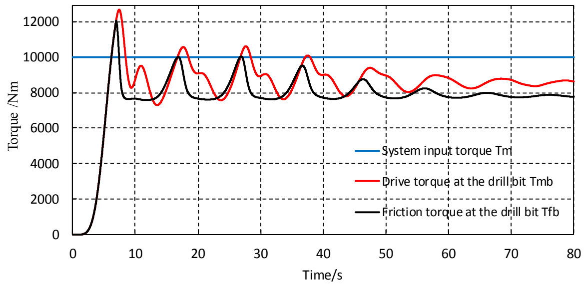

(b) With tool

Fig. 9. Torque results of drill string system with/without tool.

no new composite vibration tool, the torque of the whole drill string system increases significantly during the viscous slip process, and the range of torque fluctuation is extensive, the bit drive torque and the bit friction torque finally failed to stabilize. When there is a new composite vibration tool, however, the torque system has a small range of torque fluctuation and no stick-slip phenomenon throughout the drilling process. The friction torque of the drill bit is always sliding friction torque, and the driving torque, friction torque eventually tend to be stable.

4. Field test and analysis

To verify the feasibility and accuracy of the theoretical model and the results of the calculation example, we carried out the field experiment on the new composite vibration tool and compared the experimental field data with the results of the calcula-

Table 3. Application statistics of the composite vibration tool on the well section.

No.	Bit size (mm)	Drilling interval (m)		Drilling footage (m)	Pure drilling time (h)	ROP (m/h)
		From	To			
1	216	2318.10	2707.31	389.21	204	1.91
2	216	2707.31	2727.63	20.32	17	1.20
3	216	2727.63	2909.30	181.67	59	3.08
4	216	3065.00	3080.94	15.94	21	0.76

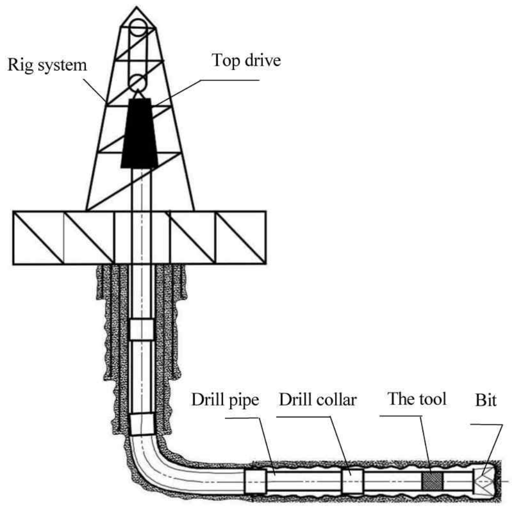

Fig. 10. Schematic diagram of the drilling system.

Fig. 11. The field test.

tion example.

A well was drilled by the field drilling team with PDC+ the new composite vibration tool, and a total of four times were drilled. The well section was 2318.10-3080.94 m, the total pure drilling time was 301 h, and the average mechanical drilling speed was 2.02 m/h. Table 2 shows the main parameters of the composite tool. Table 3 shows the specific application statistics of the tool and Fig. 11 shows the field test.

During the drilling process, the sections with/without a new composite vibration tool were compared (Figs. 12 and 13). When drilling to 3080.94 m, continue to drill after removing the new composite vibration tool. The torque fluctuation range

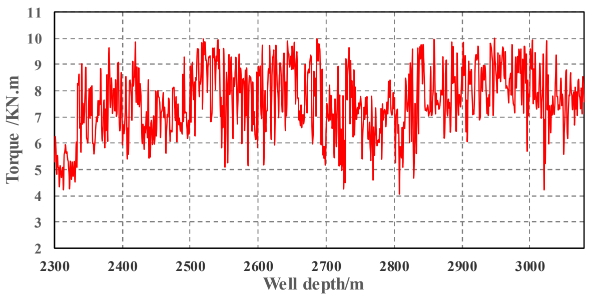

(a) With tool

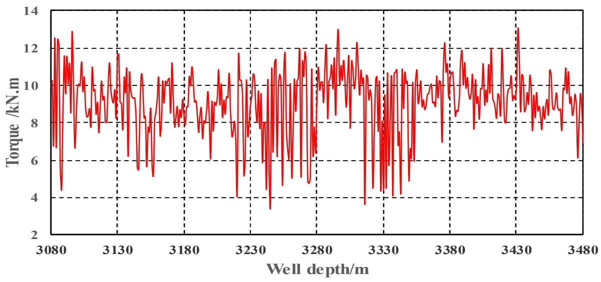

(b) Without tool

Fig. 12. Torque varies with well depth with/without tool.

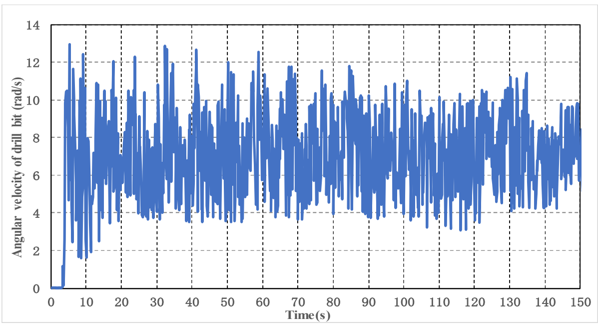

(a) With tool

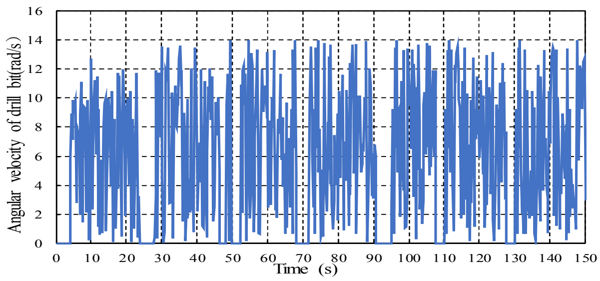

(b) Without tool

Fig. 13. Angular velocity of the drill bit with/without tool.

seen from Fig. 12(a) is small in the drilling section using the tool, which is 4.0537~9.9914 KNm, and the average torque is 7.4008 KNm. The value is close to the theoretical calculation value and within the error range. On the contrast, the torque fluctuation range of the non-tool segment is extensive, ranging from 3.5773 to 13.0132 KNm, and the average torque is 9.4914 KNm. The comparison found that the scope of torque fluctuations of the well section using the new composite vibration tool is small, the work process is stable, and the stick-slip vibration is weakened, which is consistent with the theoretical results in the overall trend. Moreover, Fig. 13 shows the angular velocity of drill bit in the field test when the new composite vibration tool is/is not available. We can see from the Fig. 13(a) that the velocity of the drill bit does not appear to be 0 when the bit starts to rotate, and the amplitude of the fluctuation gradually decreases and eventually stabilizes. We can see that the results of the angular velocity of the drill bit in Fig. 6(a) and the result of the angular velocity of the bit in Fig. 13(a) are consistent with the overall trend. Both the angular velocity at the initial moment appears as 0 and eventually stabilizes after the fluctuation. However, the velocity of the drill bit in Fig. 13(b) fluctuates greatly, and there are many stick-slip phenomena when there is no composite vibration tool in BHA. Both test results show that the new composite vibration tool can significantly reduce the stick-slip phenomenon and comparisons between the theoretical results and the experimental results further verify the correctness of the theoretical model and the example.

5. Conclusions

This paper presents a new composite tool that can generate periodic torsional vibration, then establishes torsional vibration model of drill string system including the new composite vibration tool. Based on the presented model, the dynamic characteristics of drill string are analyzed taking into account the specific downhole working conditions. By comparing the numerical analysis with field test results, it is found that the tool can significantly reduce the fluctuation range of the torque of the drill string system, improve the working stability of the drill bit and the ROP, effectively protect the BHA and prolong the service life of the drilling tool.

Based on the established torsional vibration model, we can obtain the multi-degree-of-freedom motion differential equation of the drill string system. Combining calculation parameters, the results of the angular velocity, angular displacement, phase diagram and torque with/without the new composite vibration tool are obtained. The results show that the new composite vibration tool can effectively reduce the stick-slip vibration of the drill string system.

The field experiment results verified the feasibility and accuracy of the torsional vibration model of the drill string system. The new composite vibration tool reduces the range of torque fluctuation through its circumferential vibration shock, which makes the drilling process more stable, reduces stick-slip, reduces oil exploration and mining costs, and improves economic benefits.

The detailed structural design of the new composite impactor has been completed in this paper, but the service life of the tool will affect its use value. Next, we will study the erosion, wear and fatigue failure analysis of the vulnerable parts, and the failure analysis of the powertrain as the key content to improve the engineering practical value of the tool.

Acknowledgments

All authors gratefully acknowledge the support of The State Scholarship Fund of the China Scholarship Council (CSC) (No. 201608515039), National Natural Science Foundation of China (NSFC) (No.51674216), National Science and Technology Major Project of China (No.2016ZX05038).

Nomenclature

ROP	: Rate of penetration
BHA	: Bottom hole assembly
W_{ob}	: Input static drilling pressure
T_m	: Input torque
D_i	: Drill pipe outer diameter
d_i	: Drill pipe inner diameter
l_i	: Unit drill pipe length
ρ	: Density of drill pipe material
J_i	: Moment of inertia of *i*-th node
G	: Shear modulus of drill string
ξ_{ri}	: Torsional damping coefficient per unit length
k_{ci}	: Torsional stiffness between drill pipe and drill collar
k_{cT}	: Torsional stiffness between drill collar and tool
k_{cb}	: Torsional stiffness between tool and drill bit
$k_{c(b+1)}$	: Torsional stiffness between drill bit and rock
c_{ri}	: Torsional damping between drill pipe joints
K_{ri}	: Torsional stiffness between drill pipe joints
c_{rc}	: Torsional damping between drill pipe and drill collar
c_{rT}	: Torsional damping between drill collar and tool
c_{rb}	: Torsional damping between drill collar and drill bit
$c_{r(b+1)}$	: Torsional damping between drill bit and rock

References

[1] T. G. Ritto et al., Drill-string horizon tal dynamics with uncertainty on the frictional force, *Journal of Sound & Vibration,* 332 (1) (2013) 145-153.

[2] J. Tian et al., Torsional vibrations and nonlinear dynamic characteristics of drill strings and stick-slip reduction mechanism, *Journal of Computational and Nonlinear Dynamics*, 14 (8) (2019) 081007.

[3] D. M. Lobo, T. G. Ritto and D. A. Castello, Stochastic analysis of tor sional drill-string vibrations considering the passage from a soft to a harder rock layer, *Journal of the Brazilian Society of Mechanical Sciences and Engineering*, 39 (6) (2017) 2341-2349.

[4] J. Tian et al., Rock breaking mechanism in percussive drilling with the effect of high-frequency torsional vibration, *Energy Sources, Part A: Recovery, Utilization, and Environmental Effects* (2019) 1-15.

[5] J. Tian et al., Vibration characteristics analysis and experimental study of new drilling oscillator, *Advances in Mechanical Engineering*, 8 (6) (2016) 1-10.

[6] X. Liu et al., Nonlinear motions of a flexible rotor with a drill bit: Stick-slip and delay effects, *Nonlinear Dynamics*, 72 (1-2) (2013) 61-77.

[7] B. Besselink et al., Analysis and control of stick-slip oscillations in drilling systems, *IEEE Transactions on Control Systems Technology*, 24 (5) (2016) 1582-1593.

[8] C. Song, J. Chung, J.-H. Kim and J.-Y. Oh, Design optimization of a drifter using the Taguchi method for efficient percussion drilling, *Journal of Mechanical Science and Technology*, 31 (4) (2017) 1797-1803.

[9] T. Vromen et al., Nonlinear out put‐feedback control of torsional vibrations in drilling systems, *International Journal of Robust and Nonlinear Contro*l, 27 (17) (2017) 3659-3684.

[10] S. K. Gupta and P. Wahi, Global axial-torsional dynamics during rotary drilling, *Journal of Sound and Vibration*, 375 (2016) 332-352.

[11] J. Tian, Y. Yang and L. Yang, Vibration characteristics analysis and experimental study of horizontal drill string with wellbore random friction force, *Archive of Applied Mechanics*, 87 (2) (2017) 1439-1451.

[12] Y. Liu, P. Chávez, R. De Sa and S. Walker, Numerical and experimental studies of stick-slip oscillations in drill-strings, *Nonlinear Dynamics*, 90 (4) (2017) 2959-2978.

[13] B. Besselink, N. V. D. Wouw and H. Nijmeijer, A semi-analytical study of stick-slip oscillations in drilling systems, *Journal of Computational & Nonlinear Dynamics*, 6 (2) (2011) 293-297.

[14] J. Tian et al., Working mechanism and rock-breaking characteristics of coring drill bit, *Journal of Petroleum Science and Engineering,* 162 (2018) 348-357.

[15] M. Sarker, D. G. Rideout and S. D. Butt, Dynamic model for longitudinal and torsional motions of a horizontal oilwell drill-string with wellbore stick-slip friction, *Journal of Petroleum Science and Engineering*, 150 (2017) 272-287.

[16] J. Tian et al., The wear analysis model of drill bit cutting element with torsion vibration, *Advances in Mechanical Engineering*, 7 (1) (2015) 254026, 1-9.

[17] A. Kyllingstad and G. W. Halsey, A study of slip-stick motion of the bit, *SPE Annual Technical Conference and Exhibition,* Society of Petroleum Engineers (1987).

[18] S. J. Cull and R. W. Tucker, On the modelling of Coulomb friction, *Journal of Physics A: Mathematical and General*, 32 (11) (1999) 2103.

[19] X. Liu et al., State-dependent delay influenced drill-string oscillations and stability analysis, *Journal of Vibration and Acoustics*, 136 (5) (2014) 051013.

[20] E. M. Navarro-López and R. Suárez, Practical approach to modelling and controlling stick-slip oscillations in oil well drill strings, *Proceedings of the 2004 IEEE International Conference on Control Applications*, 2 (2004) 1454-1460.

[21] E. M. Navarro-López, An alternative characterization of bit-sticking phenomena in a multi-degree-of-freedom controlled drill string, *Nonlinear Analysis: Real World Applications*, 10 (5) (2009) 3162-3174.

[22] Q. Xue et al., Modeling of torsional oscillation of drillstring dynamics, *Nonlinear Dynamics*, 96 (2019) 267-283.

[23] J. Tian et al., Analysis of stick-slip reduction for a new tor-

sional vibration tool based on PID control, *Proceedings of the Institution of Mechanical Engineers, Part K: Journal of Multi-body Dynamics* (2019) 146441931987639.
[24] J. Tian et al., Mathematical modeling and analysis of drill string longitudinal vibration with lateral inertia effect, *Shock and Vibration*, 2 (2016) 1-8.
[25] B. Besselink, N. V. D. Wouw and H. Nijmeijer, A semi-analytical study of stick-slip oscillations in drilling systems, *Journal of Computational & Nonlinear Dynamics*, 6 (2) (2011) 293-297.
[26] J. Tian, Y. Yang, L. Dai and X. Lin, Kinetic characteristics analysis of a new torsional oscillator based on impulse response, *Archive of Applied Mechanics*, 88 (10) (2018) 1877-1891.
[27] S. P. Barton, F. Baez and A. Alali, Drilling performance improve ments in gas shale plays using a novel drilling agitator device, *North American Unconventional Gas Conference and Exhibition,* Society of Petroleum Engineers (2011).
[28] J. Tian et al., Dynamic characteristics and test analysis of a new drilling downhole tool with anti-stick-slip features, *Journal of Mechanical Science and Technology*, 32 (10) (2018) 4941-4949.
[29] J. Tian et al., Vibration analysis of new drill string system with hydro-oscillator in horizontal well, *Journal of Mechanical Science and Technology*, 30 (6) (2016) 2443-2451.
[30] S. Hovda, Semi-analytical model of the axial movements of an oil-well drillstring in deviated wellbores, *Journal of Sound and Vibration,* 433 (2018) 287-298.
[31] J. Tian, L. Wei and T. Zhang, Dynamic research and experimental analysis of a new downhole drilling tool, *Arabian Journal for Science and Engineering*, 44 (12) (2019) 10231-10244.
[32] H. Qiu, J. Yang and S. Butt, Investigation on bit stick-slip vibration with random friction *coefficients, Journal of Petroleum Science and Engineering,* 164 (2018) 127-139.

Jialin Tian is currently a Professor of the School of Mechanical Engineering in Southwest Petroleum University. His research interests include mechanical nonlinear dynamics and vibration control, modern design theory and methods of oil and gas equipment, downhole tools, electromechanical system monitoring and signal analysis.

Lai Wei is currently a graduate student of the School of Mechanical Engineering in Southwest Petroleum University. His research interests include downhole tools and drilling dynamics.